Analyst

PAPER

View Article Online
View Journal | View Issue

Cite this: *Analyst*, 2019, **144**, 5589

Quantification of surface functional groups on silica nanoparticles: comparison of thermogravimetric analysis and quantitative NMR†

Filip Kunc,[a] Vinod Balhara,[a] Ying Sun,[a] Malgosia Daroszewska,[a] Zygmunt J. Jakubek,[a] Myriam Hill,[b] Andreas Brinkmann [a] and Linda J. Johnston *[a]

Thermogravimetric analysis (TGA) coupled with evolved gas analysis-FT-IR has been examined as a potential method to study the functional group content for surface modified silica nanoparticles. A comparison with a quantitative solution NMR method based on analysis of groups released after dissolution of the silica matrix is used to provide benchmark data for comparison and to assess the utility and limitations of TGA. This study focused primarily on commercially available silicas and tested whether it was possible to use a correction based on bare silica to account for the significant mass loss that occurs due to condensation of surface hydroxyl groups and loss of matrix-entrapped components at temperatures above ~200 °C. Although this approach has been used successfully in the literature for in-house prepared samples, it was problematic for commercial silicas prepared by the Stöber method. For these materials the agreement between estimates from qNMR and TGA mass loss was poor in many cases. However much better agreement was observed for samples for which the mass loss above 200 °C is relatively low, such as non-porous silica, or samples for which the mass fraction of functional group is large (*e.g.*, high molecule weight groups or multilayers). FT-IR was useful in identifying the likely structure of the components lost from the surface at various temperatures and in some cases provided evidence of contaminants in the sample. Nevertheless, in other cases correlation of thermograms and FT-IR with NMR data was necessary, particularly for samples where multi-step modification of the silica surface results in incomplete functionalization that gives a mixture of products. Overall the results indicate that TGA provides reliable results for silicas of low porosity or those for which the functional group accounts for a significant fraction of the total sample mass. It is also suitable as a supplementary or screening technique to indicate the presence of coatings or covalent surface modification, prior to applying other techniques or for routine analyses where sensitivity is not critical.

Received 12th June 2019,
Accepted 8th August 2019

DOI: 10.1039/c9an01080g

rsc.li/analyst

Introduction

Adequate physicochemical characterization of nanomaterials is essential for transferring nanomaterial research into commercial applications. Insufficient characterization makes it difficult to compare results between laboratories which hampers the establishment of quality control and risk-assessment approaches.[1] Surface chemistry is a particularly important parameter since it determines the interactions of the nanomaterial with its surroundings when incorporated into composites or devices and also when released to the environment or ingested by living organisms. Therefore, there is a need for the continued development of methods for accurate characterization of nanomaterial surfaces/coatings prior to their use for applications. Quantification of surface functional groups requires the use of multiple analytical techniques that may vary in sensitivity, range of applicability, ability to monitor accessible *vs.* total content and limitations.[2,3] Methods such as solution/solid-state quantitative NMR,[4–8] X-ray photoelectron spectroscopy,[3,9] conductometric titrations,[10] and fluorometric and colorimetric assays[11–15] have been applied but there are only a few instances where the combination of these methods is comprehensively evaluated.[3,8,11,16] As such, there is a need for the optimization and cross-validation of methods as well as a critical assessment of practical implications such as accessibility, cost, user skill required and analysis time.

[a]*National Research Council Canada, Ottawa, Ontario K1A 0R6, Canada. E-mail: linda.johnston@nrc-cnrc.gc.ca*
[b]*New Substances Assessment & Control Bureau, Health Canada, Ottawa, Ontario K1A 0K9, Canada*

†Electronic supplementary information (ESI) available: Additional results for TGA and qNMR of bare and functionalized silica nanoparticles. See DOI: 10.1039/c9an01080g

Herein, we aim to investigate the capability of TGA for the quantification of surface coatings and functional groups on silica nanoparticles (NPs) which can be readily functionalized for a variety of applications. Although TGA is not typically the primary technique for characterization of nanomaterials, it is a practical tool for industrial-scale measurements and batch-to-batch quality control and is considered a suitable initial method for assessing surface group content by OECD. In TGA the mass loss from materials is monitored as a function of temperature which yields a decomposition curve that provides parameters such as initiation/oxidation temperature or residual mass that may be indicative of material quality or the presence of impurities. This analysis has been particularly effective for the characterization of single- and multi-walled carbon nanotubes.[17,18] However, the usefulness of TGA for the analysis of other materials has been debated. For example, it has been concluded that TGA is unsatisfactory for quantification of polyethylene glycol (PEG), OH, and various organosilanes on cyanoacrylate NPs,[19] metal oxides[20] and mesoporous silicas,[21] respectively, mainly due to the overlapping decomposition of analyte and other components. On the other hand, successful quantification was reported for organosilane-modified cellulose (after correlation to elemental analysis),[22] polymer coated gold,[23] and OH quantification on silica and zirconia.[24] One drawback of TGA is the amount of material (minimum of several milligrams) needed for a single analysis which makes it less suitable for analyzing small-scale samples, thin films, or samples with minor modifications. The development by Mansfield *et al.* of microscale TGA utilizing a quartz crystal microbalance addressed this limitation, achieving good agreement with conventional TGA for PEG-modified gold/silica and layer-by-layer polymer coated gold NPs.[25]

The issue of overlapping mass loss due to surface groups and components of the material matrix is particularly problematic for silica. A number of studies have used TGA as a method to assess functional group loading or adsorbed organic materials on silica NPs;[13,26–31] most (although not all) have applied a correction for the loss of surface silanols at temperatures above ~200 °C. In most cases the correction was based on the precursor bare silica prior to functionalization. Very few of these studies have attempted to validate TGA measurements by using complementary methods to assess the reliability of the estimate obtained after correction for loss of silanols at similar temperatures to the functional group. Here we have assessed the suitability of TGA as a method for quantifying surface functional groups on silica NPs with a focus on commercially sourced materials. In order to facilitate the interpretation of decomposition curves, TGA has been coupled with Fourier transform infrared spectroscopy (FT-IR) measurements to provide information on the structure of the species removed from the surface. This so called 'evolved-gas' analysis (EGA) method was, for example, used to quantify carbon–oxygen groups generated on the sidewalls of SWNTs by ozonolyzis.[32] Quantification of surface groups by TGA has been compared to estimates obtained by a silica dissolution/quantitative NMR (qNMR) method that we have recently optimized for quantification of total functional group content on silica.[7] This approach involves dissolution of silica in basic media and subsequent quantification of the released functional groups by internal standard addition.[7,29,33] The qNMR method allows for structural identification of the functional group, an important factor when dealing with materials that have been modified using several steps. The combined information from TGA and qNMR allows us to establish general guidelines for the application of TGA to commercial silica. Our findings also highlight some of the limitations of using TGA without reference to other methods (such as FT-IR or NMR) that allow for assessment of the structure of the surface groups and interference from potential matrix components or impurities.

Results and discussion

TGA of unfunctionalized Stöber silica nanoparticles

Since the TGA results for silica prepared by the Stöber method are typically complex, we initially examined non-functionalized silica NPs from a single supplier (A, see Materials and methods) by TGA with EGA-FT-IR detection to provide a baseline for the amount and nature of components evolved at various temperatures, prior to the analysis of functionalized samples. The thermograms, differential thermograms and corresponding 3D FT-IR plots are displayed in Fig. 1 and S1† for 20, 80, 100, and 200 nm NPs. Each sample shows an initial mass loss with a maximum in the DTG curve at 100–110 °C that can be assigned to loss of water. This is followed by a mass loss that occurs between 200 and 600 °C; some samples show 2 peaks (350 and 550 °C) while others show a single maximum at ~550 °C with a broad shoulder at lower temperatures.

FT-IR spectra measured during the initial mass loss have two strong bands (4000–3000 cm^{-1} and 1900–1300 cm^{-1}) that correspond to water in the gas phase. The mass loss due to the surface water varies from 1% to 5% for the various samples, consistent with different sample histories and drying methods. Some silicas have a second component in the FT-IR spectra measured during the initial low temperature mass loss region; for example 200 nm silica (Fig. S1†) has signals at (3000–2900 cm^{-1} and 1100–1000 cm^{-1}) that suggest the presence of alcohol, most likely ethanol which is used in the synthesis and purification procedure. The presence of ethanol in unfunctionalized samples is also confirmed in ^{1}H NMR spectra after dissolution of the silica; for example, 100 nm bare silica contained 520 μmol g^{-1} ethanol which corresponds to 2.3 wt%. The effects of residual ethanol are illustrated in Fig. S2† which shows thermograms for 100 nm silica as received (dry), after freeze drying overnight and after dispersion in ethanol and drying. The amount of water decreases after freeze drying (from 1.7% to 0.8%). The sample dispersed in ethanol and then freeze-dried shows a larger mass loss (2.6%) below 200 °C and a broader peak in the DTG curve, consistent with loss of both water and ethanol. This is confirmed by the presence of an additional signal assigned to ethanol in

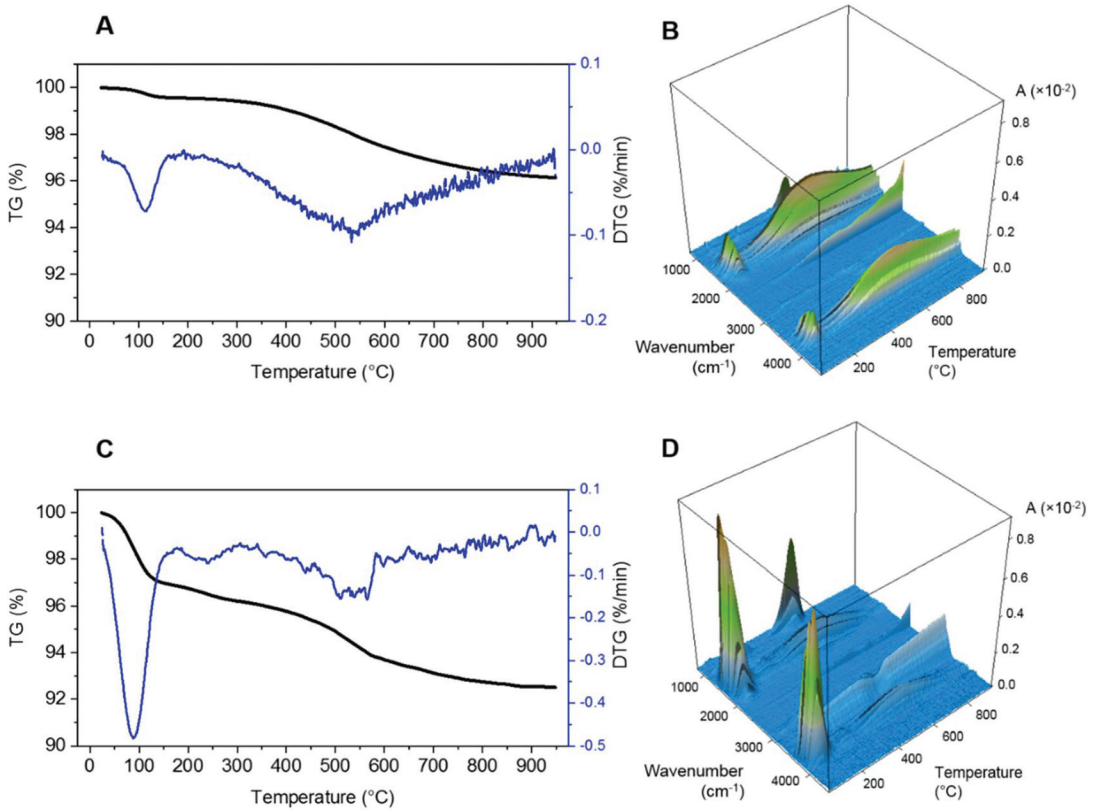

Fig. 1 Thermograms and EGA-FT-IR of unfunctionalized Stöber silica NPs analysed as received from supplier A: (A, B) 80 nm and (C, D) 100 nm. The experiments were conducted under argon with a 10 °C min^{-1} temperature gradient.

the FT-IR spectrum. However, there is minimal change in the profile for mass loss at higher temperatures suggesting that changes in storage and drying conditions affect primarily the loss of surface components at <200 °C.

FT-IR spectra recorded above 200 °C show the continuous release of water across the entire temperature gradient, consistent with previous observations of condensation of hydroxyl groups.[21] A band that matched spectra for CO_2 (2400–2350 cm^{-1}) was also observed, and its intensity increased with temperature. The presence of CO_2 can be explained by combustion of interior ethanol or ethoxy groups at higher temperatures of the thermal cycle. Although the experiments are conducted in an inert argon atmosphere, the combustion may be due to oxygen present in the system, as discussed below for polyethyleneglycol functionalized silica. A strong CO_2 band in silica samples was also observed by Li *et al.* in their recent studies of silica pore-locking mechanisms and their impact on surface area measurements by gas adsorption.[34,35] Additional bands at 950 cm^{-1} were observed at ~450 °C for 100 nm and 200 nm silica; this signal is assigned to residual ammonia, probably trapped in the silica microstructure during the synthesis.

In order to assess the variability between silica samples, multiple batches and sizes from the same producer (supplier A) were analyzed together with samples from a different supplier (B) and an in-house prepared silica (C). Samples from B (Fig. S3†) showed loss of surface water (~100 °C) and two well-resolved components at higher temperature. Unlike samples from supplier A, the thermograms had similar ratios for the two peaks at 350 °C and 550 °C for each of the 3 sizes tested. By contrast the in-house silica (C) showed primarily the lower temperature component (Fig. S3†). Table 1 summarizes the mass loss assigned to the surface components removed at low temperature and the mass loss due to hydroxyl condensation and possible removal of interior components. The data in Table S1† demonstrate that measurements on a single silica sample are repeatable with standard deviations ≈1–5% for mass loss at >200 °C. The results in Table 1 demonstrate that the mass loss at low temperature (<200 °C) assigned to surface water (or ethanol) varies by a factor of ~4, depending on the sample drying and storage conditions. The mass loss at higher temperature (>200 °C) ranges from ~2% to ~7% for the various samples. The mass loss for supplier A silica appears to increase with NP size with mass loss of 1.8–2.6% for smaller diameters (20, 50 nm) and 3.4–6.7% for larger particles (100, 200 nm). By contrast, the materials from the supplier B show no obvious trend with particle size, and are significantly larger (≈6–7%) than the mass loss from most supplier A silicas. There are batch-to-batch variations for the same size particles, independent of the sample history (see entries for supplier A in Table 1), although these are typically much smaller (<0.6%) than the variation with size or supplier.

Table 1 Mass loss observed for non-functionalized Stöber silica at low temperature (<200 °C) and high temperature (>200 °C). Samples were analyzed as received (dry powder) or after isolation from water suspension and freeze-drying

Sample, n^a	Mass loss (%) <200 °C[b]	Mass loss (%) >200 °C[b]	Sample history
A 200 nm	4.31	6.71	Dry powder as received
A 120 nm	1.40	2.77	Water, freeze dried
A 100 nm, $n = 4$	2.2 ± 0.9	3.7 ± 0.2	Dry powder as received
A 80 nm	0.69	3.25	Dry powder, vacuum dried
A 80 nm	0.83	3.17	Water, freeze dried
A 80 nm	3.51	3.60	Dry powder as received
A 50 nm	0.96	2.82	Water, freeze dried
A 20 nm, $n = 2$	1.49 ± 0.04	2.1 ± 0.4	Water, freeze dried
B 200 nm	4.4	6.8	Dry powder as received
B 100 nm	3.89	6.32	Dry powder as received
B 50 nm	4.59	7.14	Dry powder as received
C 108 nm	2.93	4.61	Water, freeze dried

[a] Sample is listed as supplier and size. The number of different lots of material (with same sample history) that were tested is listed as "n" and is 1 if not otherwise noted. [b] The standard deviation is provided for the mass loss when multiple batches were tested. The total mass loss is the sum of mass loss <200 °C and mass loss >200 °C.

As illustrated in Fig. S2,† vacuum drying is not sufficient to remove residual solvent or water and other components contributing to mass loss above 200 °C. Although it is straightforward to correct for low temperature mass loss, the significant mass loss above 200 °C is problematic for analysis of functional groups since it varies from sample to sample and will overlap with the loss of functional group. Different conditions were tested in an attempt to eliminate a larger fraction of this signal. Fig. S4† indicates that an isothermal drying step at 160 °C under an argon atmosphere for 16 h eliminated most of the components lost at <250 °C, but did not affect the mass loss at higher temperatures.

Silica prepared by the Stöber process represents a challenging material for TGA analysis since it undergoes mass loss in multiple stages. This can be attributed to the synthetic process which occurs by hydrolysis of tetraethylorthosilicate (TEOS) precursor followed by condensation to form NP nuclei. Particle growth can be controlled by the ratio of water, ethanol and ammonium hydroxide. However, depending on the reaction rate/conditions, the hydrolysis and condensation of TEOS may not be complete resulting in a partly cross-linked silica matrix that contains ethoxy groups in place of oxygen-bridged silicon atoms. Van Blaaderen *et al.* found that the content of silicon fully crosslinked *via* 4 siloxane bonds varies from 55–85% for different samples.[36] The degree of crosslinking can be even lower in particles prepared by microemulsion, where 3% of silicon atoms are bridged by only 2 siloxane bonds. Several recent reports have concluded that there are micropores (diameter ~1 nm) in Stöber silica.[34,35,37] These micropores can presumably trap components from the synthesis such as water, ethanol and ammonia, the loss of which may overlap with release of water from the condensation of neighboring free hydroxyls. For a specific sample some or all of the above factors will be convoluted with the mass loss due to the functional group which may have only a minor contribution to the thermogram.

Quantitative NMR for measuring functional group content

Solution ^{1}H NMR was employed for the quantification of the total amount of functional group in various silica samples that were used for TGA analysis. The optimization and the applicability of this method for the quantification of amine functional groups on silica NPs is described in our previous work.[7] Therein we demonstrated that amines can be reliably detected and quantified by ^{1}H qNMR after the complete disintegration of the silica matrix in basic solution which liberates functional groups in close to monomeric form. The utility of the qNMR method has been demonstrated in several other studies.[29,33] The dissolution protocol was optimized for other functional groups including carboxylic acids, thiols, imidazolines and PEG and for silicas prepared by several methods, as outlined in the Materials and methods. Quantification using an internal standard (typically potassium hydrogen phthalate) requires that the analyte resonances are well-resolved and can be confidently assigned to the functional group. An example for quantification of the imidazoline moiety by the silica dissolution/qNMR method is shown in Fig. 2 and additional examples are provided in Fig. S5.† In the case of PEG ^{1}H NMR spectra allow the determination of the average molecular weight of the chain by comparing the integral of ethylene glycol chain with the integral of terminal –CH_3/Si–CH_2–.

Functionalized Stöber silica NPs

To assess the impact of loss of silica matrix components on functional group quantification by TGA, functionalized samples of 20–200 nm diameter NPs were analyzed. Most samples were modified with 3-aminopropyl siloxanes which is one of the most frequent treatments for introducing reactive surface groups and improving dispersibility. In our previous study, two solution colorimetric assays and solid-state qNMR and X-ray photoelectron spectroscopy of fluorinated-probe-labelled silicas were employed to quantify the reactive, surface accessible amines on silica NPs. The results were compared to total amine content measured by silica dissolution and qNMR in solution.[8] Representative results for TGA of two aminated silicas are shown in Fig. 3. The thermograms show loss of water and ethanol at temperatures <300 °C, as evidenced by FT-IR signals. Note that all the aminated samples show loss of ethanol at higher temperatures than the bare samples; this may correspond to nonhydrolysed ethoxy groups on APTES. For each sample there is a relatively large mass loss with a maximum in the differential TGA curve at 530 °C. This corresponds to an additional signal at 2880–3180 cm^{-1} in the FT-IR which may be due to amine loss.

Quantification of amine loss requires correction for loss of components from bare silica. As shown above, the mass loss above 200 °C varies with sample batch, supplier and particle size, presumably due to variability in the synthesis process.

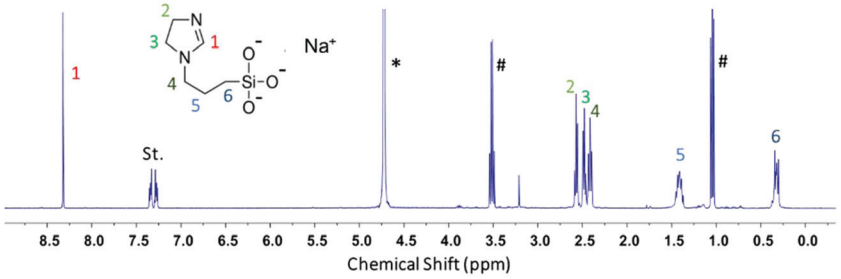

Fig. 2 A representative ^{1}H NMR spectrum obtained after dissolution of 200 nm silica NPs functionalized with an imidazoline moiety. Resonances (1–6) are assigned as shown on the structure and normalized integrals are averaged and compared to the internal standard (St, potassium phthalate monobasic). Water and ethanol signals are marked with * and #, respectively.

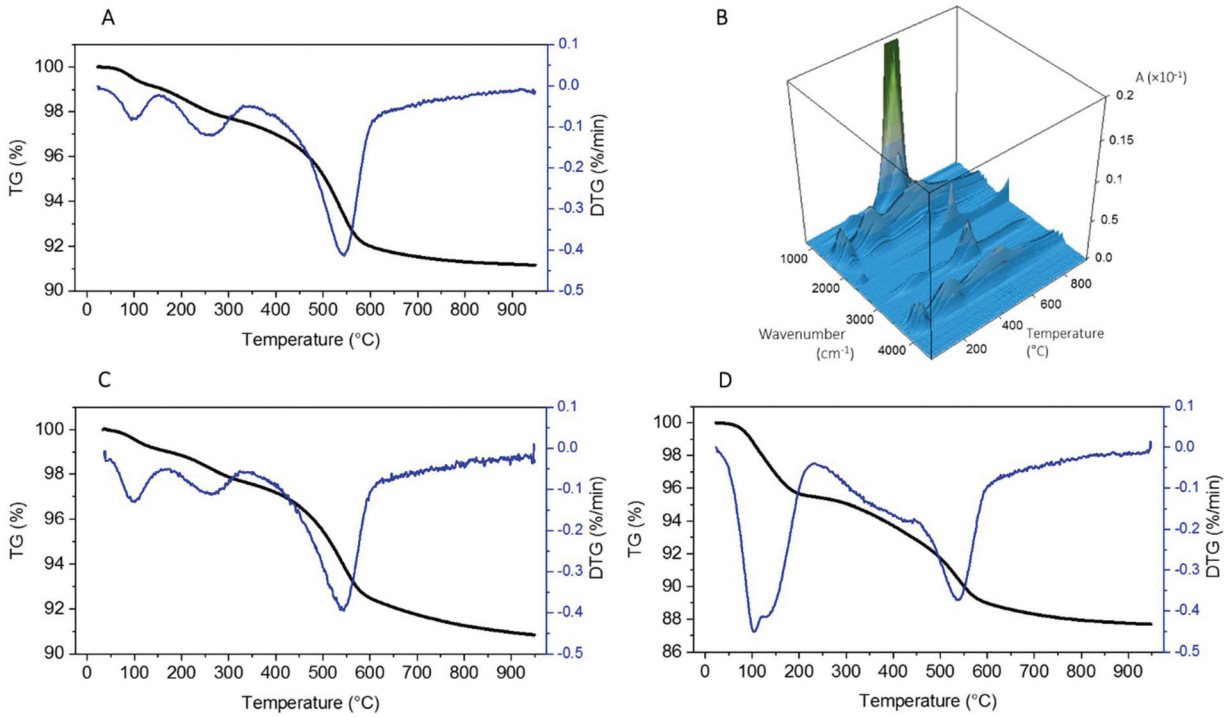

Fig. 3 Thermograms of amine functionalized NPs: (A) 80 nm $SiO_2C_3NH_2$ (supplier A) with corresponding EGA-FT-IR (B), (C) 100 nm $SiO_2C_3NH_2$ NPs (supplier A), (D) 200 nm SiO_2@C_3NH_2 NPs (supplier B).

Since it is not typically feasible to correct for the bare sample used for surface functionalization with commercial samples, we tested whether the average mass loss for the same NP size from the same supplier could be used as a correction. Table 2 shows the results of quantification of amine groups on silica NPs by qNMR and TGA. The TGA results have been obtained from the total mass loss after subtracting the solvent contribution (typically <~200 °C) and correcting for the mass loss above 200 °C for a silica sample of the same size. In some cases the correction for mass loss of bare silica was based on the average of several batches for that size (see Table 1). The results for supplier A silica NPs indicate that the amount of functional group calculated by TGA is 3–4 times higher than the total amine content measured by qNMR for several batches of 80 and 100 nm NPs. By contrast, for 20 nm NPs TGA estimates a ~20% lower amine content than qNMR. The smaller NPs have the lowest correction for mass loss above 200 °C for bare particles and the highest amine content (expressed as μmol g^{-1} silica) owing to their high surface to volume ratio. This may explain why the TGA estimate is similar to the qNMR value. Note that qNMR is the more reliable method by virtue of its chemical identification capabilities, which provide additional confidence in the quantification.

For comparison TGA was used to estimate the functional group content for a PEGylated silica from supplier A and several functionalized silicas from supplier B. The qNMR and TGA estimates are in good agreement for the PEGylated sample, consistent with the high molecular weight of the

Table 2 Quantification of silica functional groups by qNMR and TGA before and after correction for bare non-functionalized NPs of similar size. Standard deviations for multiple batches of silica are provided for some qNMR measurements

Sample	qNMR (μmol g^{-1})	TGA, corrected (μmol g^{-1})	TGA, uncorrected (μmol g^{-1} (wt%))
A 100 nm C_3NH_2	130	262[a]	948 (5.40%)
A 100 nm C_3NH_2	180 ± 2[b]	674	1380 (7.98%)
A 100 nm C_3NH_2	180 ± 2	686	1415 (8.21%)
A 80 nm C_3NH_2	130 ± 2	592	1190 (6.90%)
A 80 nm C_3NH_2	127 ± 3	345	915 (5.32%)
A 20 nm C_3NH_2	655 ± 3[b]	545	900 (5.22%)
A 120 nm PEG	121	109	150 (10.99%)
B 200 nm C_3NH_2	267 ± 16	167	1340 (7.79%)
B 200 nm C_3SH	402 ± 1	320	1230 (9.24%)
B 200 nm C_3-imidazoline	562 ± 3	386	999 (11.00%)

[a] This value is the mean of two replicates measured to maximum temperatures of 800 °C and 950 °C; the standard deviation for the 2 replicates is ±5 μmol g^{-1}. [b] From ref. 7.

polymer (733 g mol^{-1}), which means that variations in the correction have relatively low impact. The agreement between methods for the 3 silicas from supplier B is less good; TGA estimates are 20–37% lower than the qNMR values, indicating that the bare silica correction is an overestimate by contrast to the results for most supplier A samples. Supplier B silicas have a high amine content, as much as six times higher than the estimated monolayer coverage of 92 μmol g^{-1} for NPs with an average diameter of 200 nm; this estimate is based on the surface area calculated from the average particle diameter and a silica density of 1.96 m^2 g^{-1} and assumes 4 aminopropyl siloxane moieties per nm^2 as the closest possible packing of functional groups on the surface.[38] Overall these results indicate that TGA agrees reasonably well with total amine content measured by qNMR for samples which have a high molecular weight functional group or a high amine content such as small high surface area NPs or NPs with amine multilayers.

The large difference between TGA and qNMR estimates for 80 and 100 nm NPs aminated NPs from supplier A is unlikely to be accounted for by batch-to-batch variability of the bare silica used for correction purposes. One possible explanation for this discrepancy could be differences in the functionalization procedure. It is known that treating surfaces with APTES can result in disordered layers with potential vertical polymerization of APTES. Depending on the reaction conditions, the hydrolysis of ethoxy functional groups may be incomplete, and APTES can be immobilized through only one or two siloxane bonds. The presence of residual ethoxy groups on the newly formed amine layer would have considerable impact on TGA interpretation. For example, the contribution of one non-hydrolyzed ethoxy group from each immobilized APTES molecule in the mass loss would decrease the calculated amine content by 0.56×. However, this cannot account for the full extent of the discrepancy, indicating that additional differences in matrix effects must contribute. The presence of an impurity from the synthesis is one possibility. However, the qNMR spectra provide no evidence for impurities, although ethoxy groups would not be detected in the presence of the substantial amounts of ethanol that are observed for the silica NPs. Finally, the surface functionalization process may result in a larger amount of residual solvent within the silica microstructure compared to the initial unfunctionalized material.

One recent study employed TGA and qNMR for quantification of surface groups on in-house synthesized silica NPs and found good agreement between the two methods, after correcting for mass loss of unfunctionalized particles.[29] The authors stressed the importance of determining the correction for the batch of bare particles subsequently used for functionalization. As shown here such an approach is typically not routinely feasible for commercial materials.

TGA of non-porous silica NPs

Recent studies have provided evidence for a significant level of porosity for Stöber silicas and demonstrated that variations in washing and drying steps influence the microporous structure, leading to trapping of solvent and other components.[34,35,37] Therefore, we examined samples of a commercial non-porous silica prepared by a modified Stöber process that includes a calcination step; we reasoned that the lower porosity would reduce the magnitude of the correction for water and other components. Samples of 30–100 nm diameter silicas from supplier D gave thermograms (Fig. S6†) with a small mass loss due to solvent at low temperature and a broad mass loss (1–1.6%) above 200 °C (Table 3) that was approximately a factor of two lower than that for most of the Stöber silicas in Table 1. This is consistent with a lower porosity for supplier D silicas which is anticipated to improve the reliability of TGA measurements of functional group content. Non-porous silicas with three different functional groups (PEG, C_3NH-succinate, $C_{11}CO_2H$) were studied by TGA, as summarized below. These results illustrate the utility of TGA coupled with FT-IR for identifying functional groups as well as some of the limitations in analyzing more complex functional groups and samples with impurities.

SiO_2-PEG. Samples of 30 and 50 nm PEG modified silica show loss of a small amount of water (<200 °C), followed by a single large mass loss (500 °C) that can be assigned to the functional group (Fig. S7†). The FT-IR spectrum recorded at 500 °C has signals due to water and CO_2 that correspond to

Table 3 Mass loss observed in nonfunctionalized non-porous silica NPs

Sample	Mass loss (%) <200 °C	Mass loss (%) >200 °C
D 30 nm	1.60[a]	1.64[a]
D 50 nm	1.48	1.55
D 75 nm	1.26	1.21
D 100 nm	1.08	1.09

[a] Standard deviations for 3 replicates are 0.24 and 0.06 for mass loss at <200 °C and >200 °C, respectively.

Table 4 Comparison of TGA/qNMR quantification of PEG, 3-aminopropylsuccinate and dodecanoic acid modified silica NPs (supplier D). For the dodecanoic acid modified silica, only the ≈300–520 °C region of the thermogram was assigned to the functional group based on the FT-IR analysis in Fig. 5. All samples were corrected for mass loss in bare silica of a similar size

Sample	qNMR (μmol g^{-1})	TGA, corrected (μmol g^{-1})	TGA, uncorrected (μmol g^{-1} (wt%))
D 30 nm PEG	201 ± 21	230	260 (12.80%)
D 50 nm PEG	121 ± 4	123	150 (7.37%)
D 37 nm 3-amino-propylsuccinate	Amino-succinate: 399 ± 4	341[a]	406 (7.19%)
	Amine: 174 ± 5	420[b]	499 (7.19%)
D 30 nm C_{11}COOH	210 ± 1	133	521 (3.80%)
D 50 nm C_{11}COOH	221 ± 11	180	752 (4.21%)
D 100 nm C_{11}COOH	129 ± 1	120	210 (2.89%)

[a] Assuming loss of 3-aminopropylsuccinate. [b] Assuming loss of a 3 : 7 mixture of propylamine and 3-aminopropylsuccinate.

loss of the PEG moiety. Quantification of the amount of functional group from the TGA mass loss for 30 and 50 nm PEG-modified silica (Table 4) gives values that are in good agreement with the estimates from qNMR, as might be anticipated from the large mass loss. Despite this good agreement, the observation of CO_2 is a potential cause for concern, as the source of oxygen is not obvious and may have to be taken into account for quantification purposes. Therefore, the samples were also analyzed using the same thermal gradient in an air atmosphere. The thermogram changed significantly with mass loss occurring at lower temperatures and the appearance of additional signals in the FT-IR spectra (Fig. S7D†). However, the total mass loss was almost identical for air and argon atmospheres (13.07% and 13.19% for air and argon, respectively). This leads to the conclusion that the oxidation occurs inside the TGA after the initial loss from the sample, probably within the silica-lined tubing that connects the TGA to the FT-IR detector. The tubing is maintained at 200 °C, which can lead to condensation of less volatile components released above 200 °C, and may provide a reservoir for residual oxygen from previous analyses, despite the use of argon as the carrier gas. A similar conclusion was reported in a recent study by Gu *et al.* who also observed CO_2 signals in TGA EGA-FT-IR of silica performed under an argon atmosphere.[35] It should be noted that only volatile compounds (boiling point <200 °C) will be detected by EGA-FT-IR.

SiO_2C_3NH-succinate. An example of the more complex 3D FT-IR spectra for silica NPs modified with a succinate is shown in Fig. 4. This commercial sample was prepared from 3-amino-

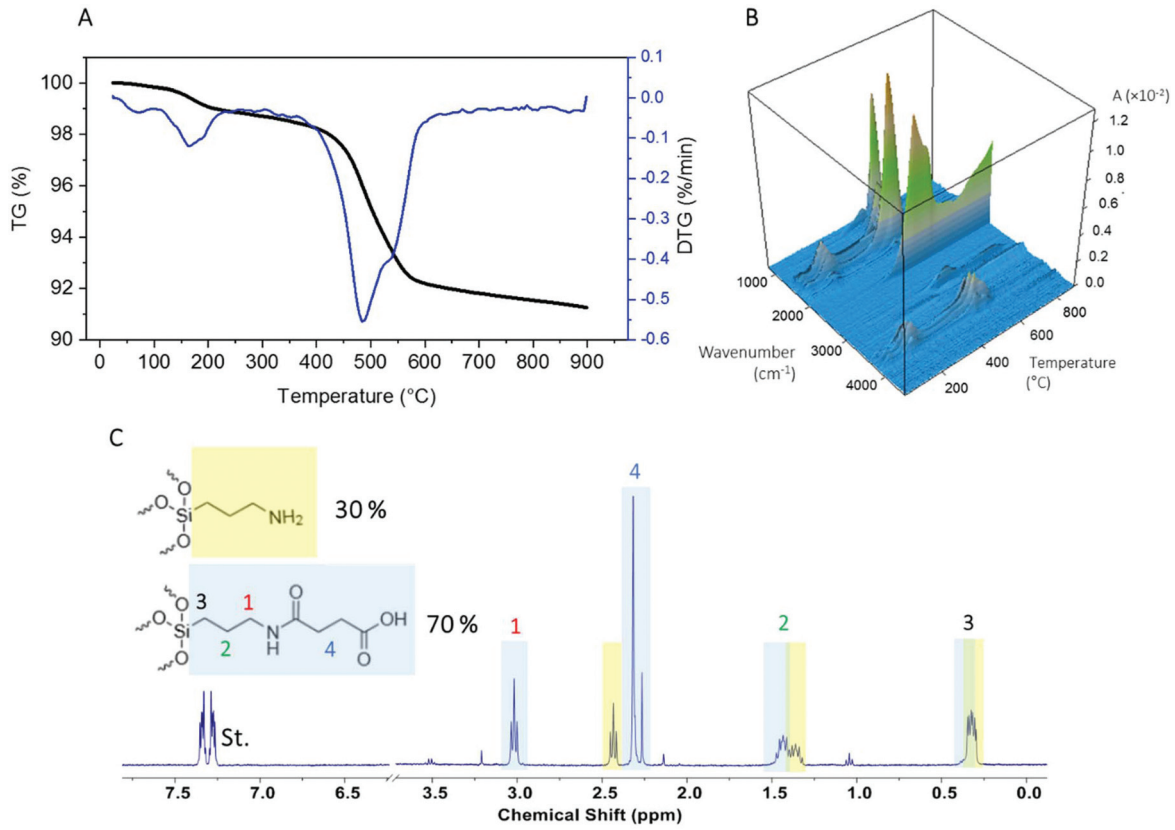

Fig. 4 37 nm SiO_2C_3NH-Succinate NPs: (A) thermogram with corresponding EGA-FT-IR (B), (C) solution ^1H NMR spectra (internal standard potassium phthalate at 7.30 ppm). The splitting of aminopropyl resonances suggests partial functionalization with succinate, which can be quantified from resonance (4). This signal is due to bound succinate and free succinic acid produced by hydrolysis under the dissolution conditions (0.4 M NaOD). Further details on the spectral interpretation are provided in Fig. S9.†

propyl functionalized silica by reaction with succinic anhydride to provide an amide terminated with a carboxylic acid group. The thermogram shows loss of water, followed by a large mass loss at ~480 °C; FT-IR plots (Fig. 4) show signals due to CO_2 and H_2O (indicative of combustion) as well as the presence of compounds containing a carbonyl group. At higher temperature components that match reference spectra of unsaturated molecules containing oxygen (Fig. S8†) are observed. These signals indicate that the observed mass loss of 6.04% (after correction for bare NPs) is consistent with the structure of the functional group, although it is not possible to distinguish whether loss of the functional group occurs in one or two steps.

The comparison to qNMR analysis is not straightforward for the succinate-modified silica. The ^{1}H NMR spectrum of the dissolved silica shows a mixture of signals that can be assigned to the initial primary amine and the amide formed by addition of succinic anhydride. The signal assignment was confirmed based on a control reaction of APTES and succinic anhydride in D_2O and 0.4 M NaOD (Fig. S9†). NMR quantification of the two components indicates that the sample contains ≈30% of unreacted primary amines. This is an important consideration for the interpretation of TGA analysis which depends on the precise knowledge of the analyte's molecular weight. Table 4 shows the results of qNMR analysis and the outcomes of two different interpretations of the TGA results. If the observed mass loss (6.04%, after correction for bare silica) is assumed to correspond to the expected functional group (propylamine quantitatively modified with a succinate moiety), a functional group content of 341 μmol g^{-1} is obtained. This is considerably lower than the amount of succinate determined by NMR (399 μmol g^{-1}). Recalculation using the average MW based on 70% amine modification gives a higher value of 420 μmol g^{-1}; however, this is still lower than the total functional group content (*i.e.*, primary amine + succinate) of 573 μmol g^{-1}. This example illustrates the limitations of TGA for quantification of samples which have been modified in a two-step process that leads to a mixture of products.

$SiO_2C_{11}COOH$. Three sizes of silica NPs functionalized with dodecanoic acid were examined. The DTG curve in Fig. 5A shows that the mass loss for the 30 nm NPs occurs at 495 °C and 570 °C, in addition to a small loss of water at lower temperature. FT-IR indicates that the first peak is an unsaturated alkyl chain (3100–2700 cm^{-1} – Fig. S10A†), consistent with loss of the carboxylic acid functional group. The mass loss at 570 °C corresponds to material with a strong IR band between 1100–1200 cm^{-1}. Similar bands were observed in the FT-IR spectra of the 50 and 100 nm samples (Fig. S10†); note that the mass loss at 570 °C varies considerably for the 3 different samples. The mass loss corresponding to the first peak

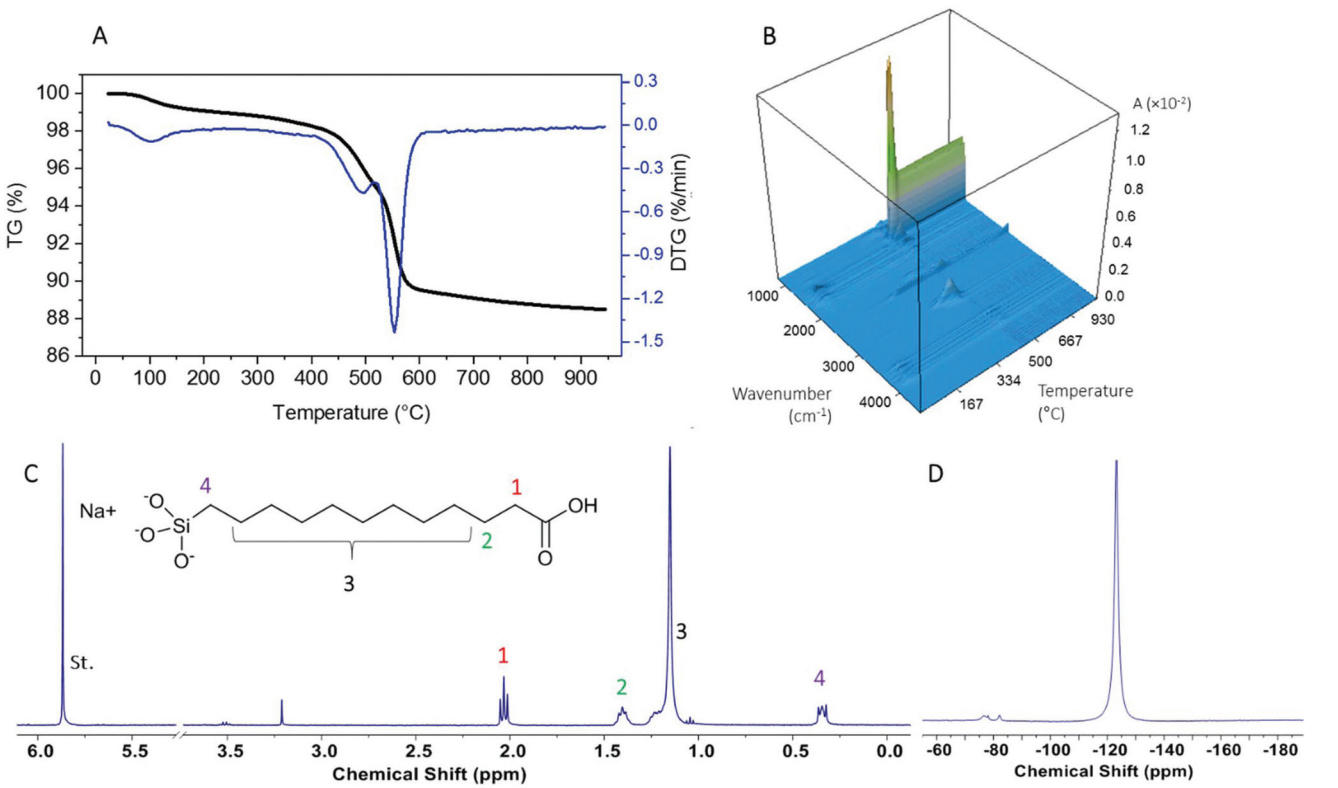

Fig. 5 Characterization of 30 nm $C_{11}COOH$ modified silica NPs s: (A) thermogram, (B) EGA-FT-IR, (C) solution ^{1}H NMR spectra (internal standard maleic acid at 5.90 ppm), (D) solid state ^{19}F NMR spectra. Note that the 1100–1250 cm^{-1} bands in the FT-IR spectra have maximum intensity at 550 °C and continue to be detected until the end of the temperature gradient. This implies that the released polyfluorinated hydrocarbon condenses in the transfer line (200 °C) and continues to be released by argon flow despite the lack of further mass loss in the thermogram.

(495 °C) corresponds well to the amount of functional group measured by qNMR (Table 4) for both the 50 and 100 nm silicas, although the TGA estimate based on this peak is ~30% too low for the 30 nm silica; including the mass loss due to both peaks would overestimate the functional group content by as much as a factor of 3 for these 3 samples. This suggests that the second peak may be an impurity and several experiments were carried out to confirm this hypothesis.

First the TGA was repeated in an air atmosphere which, as shown above for PEG-functionalized silica, can facilitate combustion of the functional group at lower temperature. This resulted in loss of the 495 °C component and a new peak at lower temperature with a similar mass loss, but little or no change in the position of the 570 °C peak (Fig. S11†). The results at a slower temperature gradient were similar. The mass loss of the unknown impurity at 570 °C was not altered in an air atmosphere (Table S2†); however, FT-IR indicated that it was transformed to CO_2 implying that the impurity contains carbon and is incorporated inside the silica matrix.

Secondly, the ^{1}H NMR spectrum obtained after dissolution of the dodecanoic-functionalized silica NPs shown in Fig. 5C matched the anticipated structure of the functional group and provided no evidence for an impurity. The FT-IR spectra for the mass loss at 570 °C were similar to fluorinated hydrocarbons, particularly tetrafluoroethene. Tetrafluoroethene and its oligomers are known to be thermal decomposition products of polytetrafluoroethylene.[39] Although perfluorinated alkenes would not be detectable by ^{1}H NMR, both ^{19}F and ^{13}C solution NMR failed to provide evidence for such an impurity. However, the presence of a fluorine-containing component was confirmed by ^{19}F solid-state NMR (Fig. 5D). The spectrum shows weak resonances at −80 ppm and a strong resonance at −125 ppm, that can be assigned to CF_3 and CF_2 groups, respectively, consistent with the presence of perfluoroalkyl chains in the sample. Since the solution NMR method requires solubilization of the silica matrix in basic D_2O, the absence of solution NMR signals can be explained by the hydrophobicity of polyfluorinated alkenes which are insoluble in water. This example highlights the importance of a multi-technique approach for the characterization of commercial nanomaterials. TGA coupled with FT-IR was adequate for functional group identification and quantification as confirmed by solution qNMR. However, solid state NMR was required to confirm the presence and structure of the impurity.

Materials and methods

Materials

Deuterium oxide (99.9%), sodium deuteroxide (10 M in D_2O), 3-aminopropyltriethoxyilane (99%, APTES), succinic anhydride (99%), tetraethyl orthosilicate (TEOS) (99.99%), ammonium hydroxide solution (28% w/v in water, ≥99.99%), TraceCERT maleic acid (99.94% maleic acid mass fraction), and TraceCERT potassium phthalate monobasic (99.92% mass fraction) were purchased from Sigma-Aldrich.

Silica NPs were acquired from three different manufacturers: NanoComposix (supplier A), Superior Silica (supplier B) and Applied Quantum Materials (supplier D). According to the manufacturer information, samples from supplier A were modified with silanes after the synthesis of the NP core. Samples from suppliers B and D were prepared by the Stöber and a modified Stöber process that includes a calcination step, respectively. Samples prepared in house (supplier C) were synthesized by stirring TEOS and ammonium hydroxide in anhydrous ethanol for 16 h and were purified by centrifugation and redispersion in ethanol (3×) and water (1×). Bare silica NPs were received and stored as dry powders or water dispersions. Prior to analysis, NPs stored in water dispersions were isolated by centrifugation and freeze-dried for 16 h. Functionalized silica NPs were received as dry powders or ethanol dispersions. Prior to analysis, NPs in ethanol dispersions were washed by resuspending and centrifugation in deionized water (1×) and freeze-dried for 16 hours. DiaTEC Reload (Diamed, CA) pipet tips were used throughout.

Sample preparation for ^{1}H qNMR

Samples were prepared according to the procedure described in our previous study.[7] Briefly, 3–12 mg of dry silica was dispersed in NaOD (0.65 mL, 0.4 M in D_2O) in a microcentrifuge tube (Eppendorf 1.5 mL safe-lock, Fisher Scientific). The closed microcentrifuge tube was placed in a Ther-Mix heated mixer (Vitl Life Science Solutions) and shaken at 1200 RPM at 45 °C for 3 hours for samples from supplier A, B and C, and for 16 hours for supplier D samples (which were less easily dispersed). The sample was cooled to room temperature and an exact mass of D_2O solution of internal calibrant was added; the calibrant solution was prepared gravimetrically and an appropriate amount was added to ensure that the ratio of integrals for unknown to calibrant was between 5 and 0.2. For a sample with ~10 mg of dissolved silica, 0.24–0.26 mg of potassium hydrogen phthalate was used. The sample was vortexed for 5 s and transferred to a standard borosilicate NMR tube (5 mm).

Quantitative ^{1}H NMR

All experiments were performed at 20 °C (±1 °C) with a Bruker Avance III 400 MHz spectrometer equipped with a 5 mm BBFO probe. For each analyte sample, the 90°pulse width was calibrated by determining the null signal generated by a 360° pulse width divided by 4 (in μs). The spin-lattice-relaxation time (T_1) was measured using an inversion-recovery experiment for each resonance of the analyte and the calibrant (potassium phthalate monobasic or maleic acid), and a delay of at least 7× the longest relaxation time for the components in the mixture was used (note: T_1 can vary from <1 s in alkyl chains hydrogens up to 21 s in imidazoline). The maximum value for the receiver gain was obtained. The ^{1}H NMR spectrum was then recorded using the 90° pulse program with the following parameters: 2 dummy transients, 32 transients, and 12 ppm spectral width with 4 ppm transmitter offset. The acquired FIT spectra were processed by Fourier transformation and phase- and baseline-corrected manually by a fifth-order polynomial fit.

^{19}F solid state NMR

A Bruker 200 MHz Avance solid state NMR spectrometer equipped with a 3.2 mm Bruker double resonance probehead and magic-angle spinning at a frequency of 18 kHz were used for all experiments. Silica NPs (~8 mg) were placed in the sample rotor. The probe was tuned to the ^{19}F Larmor frequency given by 188.7 MHz prior to every measurement. The published protocol for ^{19}F solid-state qNMR[40] was employed, specifically metrological traceability was achieved by using 3,5-bis(trifluoromethyl)benzoic acid (BTFMBA) as external calibrant. Furthermore, we employed the ERETIC (Electronic REference To access *In vivo* Concentrations) and EASY (Elimination of Artifacts in NMR Spectroscopy) methods.[41,42] A relaxation delay of 20.89 s and a spectral width of 100 kHz were used for all experiments. We co-added 3328 individual transients with 4096 complex data points and identical receiver gain. The 90° pulse was optimized on both the calibrant and analyte samples which in both cases were found to be 2.8 μs.

TGA experiments

Experiments were conducted using either a NETZSCH Iris TG209 F1 or a NETZSCH Jupiter STA449 F1 instrument coupled with a Bruker Tensor 27 FT-IR spectrometer. Temperature and mass calibrations were done as recommended by the manufacturer. In a typical experiment, 20–40 mg of powdered sample was loaded to an empty aluminum oxide crucible that was pre-treated by annealing in a natural gas flame for approximately 30 s. The mass of sample was adjusted to ensure that a total mass loss of at least 1 mg was obtained. The sample was inserted into the instrument under 50 mL min^{-1} argon atmosphere (argon protective 25 mL min^{-1}) and left to stabilize the mass for 1 hour; the transfer line to the FT-IR is also purged with the same flow of argon. The thermal cycle 25 °C–950 °C (10 °C min^{-1}, unless otherwise specified) was then initiated maintaining the same argon flow. For FT-IR results the residence time in the transfer line is ~2.5 s. All TGA experiments were run against the correction for an empty aluminum oxide crucible in argon atmosphere. Thermograms were processed by first excluding the mass loss below ~200 °C due to water and/or ethanol. Note that the temperature at which the first derivative curve reaches a minimum varied somewhat from sample to sample, depending on the amount of solvent in the sample. The mass loss above 200 °C for a sample of similar size from the same supplier was used to correct the observed mass loss in the functional group region. An example of the correction procedure is provided in Fig. S12.† The mass loss due to an impurity (where identified) was excluded from the quantification of the functional group. All mass loss values are expressed as wt%.

Conclusions

The results have shown that the mass loss measured by TGA for bare silica NPs is variable, and may be as high as 10% in agreement with previous studies. This introduces significant issues in employing TGA as a method to quantify surface group loading in modified silicas. Although it is relatively easy to correct for the loss of solvent (typically water or ethanol) at temperatures below 200 °C, the correction for mass loss at higher temperatures is more problematic, since it occurs in the same range as covalently attached functional groups. The mass loss above 200 °C varies when comparing materials from different suppliers, and is significantly higher for Stöber silica compared to a less porous alternative prepared by a modified Stöber process. The mass loss from Stöber silica can be assigned to condensation of surface hydroxyl groups as well as contributions from solvent or other materials (*e.g.*, ammonia or ethoxy groups) trapped within the microporous structure, as demonstrated in several recent studies that have shown that synthetic conditions and aging of the sample have significant effects on silica microporosity.[34,35,37] The large mass loss from the silica matrix and its lack of reproducibility from sample to sample for Stöber silicas make it challenging to use TGA to estimate functional group content for surface-modified silicas. Corrections based on mass loss from a similar size NP frequently provide results that agree very poorly with total functional group content measured by qNMR. In principle these issues may be less problematic for cases where the functional groups are added by modification of preformed bare silica which can be used for correction purposes. However, this is not often feasible for commercial samples. The studies summarized herein demonstrate that the accuracy of TGA quantification can be improved in the following cases: (1) the template bare silica does not show significant mass loss after the removal of surface associated components (typically <3%, as for non-porous silicas prepared by a modified Stöber process), and (2) the mass fraction of the functional group is relatively large, due to either a high total content (*e.g.*, multilayers) or a high molecular weight (*e.g.*, PEG). For non-porous silica with a mass loss of 1.5% or less due to water and matrix components, we estimate that a mass loss of functional group of 1 mg is adequate for reliable quantification. This corresponds to a surface loading of ~50 μmol for a $C_{11}CO_2H$ functional group.

The FT-IR detection of evolved gas is useful for the identification of the species produced during TGA and can help to identify contaminants. However, the interpretation of 3D FT-IR spectra requires caution and may require comparison of argon and air atmosphere. It is noteworthy that combustion may occur even in argon atmosphere effectively transforming useful diagnostic signals to CO_2. Some of the commercial samples examined had complex surface chemistry related to multi-step reactions and contaminants. TGA alone cannot tackle such challenges and must be coupled with other methods such FT-IR or NMR.

In conclusion, TGA is well suited as a screening technique to indicate the presence of coatings or covalent surface modification of silica NPs, but accurate quantification may require other methods. Alternatively, TGA may also be useful for routine analysis of samples with high loadings where sensitivity is not critical. Although qNMR has advantages for quantification of total functional group content, this method

is less generally accessible, particularly in industrial labs, and is more expensive and time-consuming than TGA. Studies such as the present comparison are expected to be useful in providing guidance as to the range of applicability of the various surface characterization methods.

Conflicts of interest

There are no conflicts of interest to declare.

Acknowledgements

Support for this work from the Natural Sciences and Engineering Research Council (student stipend) is gratefully acknowledged. We thank Applied Quantum Materials staff for helpful discussions on silica synthesis.

References

1 H. F. Krug, *Angew. Chem., Int. Ed.*, 2014, **53**, 2–18.
2 D. R. Baer, *Front. Chem.*, 2018, **6**, 145.
3 A. Hennig, P. M. Dietrich, F. Hemmann, T. Thiele, H. Borcherding, A. Hoffmann, U. Schedler, C. Jäger, U. Resch-Genger and W. E. S. Ungera, *Analyst*, 2015, **140**, 1804–1808.
4 N. Kong, J. Zhou, J. Park, S. Xie, O. Ramstrom and M. Yan, *Anal. Chem.*, 2015, **87**, 9451–9458.
5 S. E. Lehman, Y. Tataurova, P. S. Mueller, S. V. Mariappan and S. C. Larsen, *J. Phys. Chem. C*, 2014, **118**, 29943–29951.
6 S. K. Davidowski and G. P. Holland, *Langmuir*, 2016, **32**, 3253–3261.
7 F. Kunc, V. Balhara, A. Brinkmann, Y. Sun, D. M. Leek and L. J. Johnston, *Anal. Chem.*, 2018, **90**, 13322–13330.
8 Y. Sun, F. Kunc, V. Balhara, B. Coleman, O. Kodra, M. Reza, M. Chen, A. Brinkmann, G. P. Lopinski and L. J. Johnston, *Nanoscale Adv.*, 2019, **1**, 1598–1607.
9 M. W. Ambrogio, M. Frasconi, M. D. Yilmaz and X. Chen, *Langmuir*, 2013, **29**, 15386–15393.
10 S. Kralj, M. Drofenik and D. Makovec, *J. Nanopart. Res.*, 2011, **13**, 2829–2841.
11 M. Moser, N. Nirmalananthan, T. Behnke, D. Geibler and U. Resch-Genger, *Anal. Chem.*, 2018, **90**, 5887–5895.
12 H. Ritter and D. Bruhwiler, *J. Phys. Chem. C*, 2009, **113**, 10667–10674.
13 J. M. Rosenholm and M. Linden, *Chem. Mater.*, 2007, **19**, 5023–5034.
14 E. Soto-Cantu, R. Cueto, J. Koch and P. S. Russo, *Langmuir*, 2012, **28**, 5562–5569.
15 I.-L. Hsiao, S. Fritsch-Decker, A. Leidner, M. Al-Rawi, V. Hug, S. Diabate, S. L. Grage, M. Meffert, T. Stoeger, D. Gerthsen, A. S. Ulrich, C. M. Niemeyer and C. Weiss, *Small*, 2019, **15**, 1805400.
16 A. Hennig, H. Borcherding, C. Jaeger, S. Hatami, C. Wurth, A. Hoffmann, K. Hoffmann, T. Thiele, U. Schedler and U. Resch-Genger, *J. Am. Chem. Soc.*, 2012, **134**, 8268–8276.
17 E. Mansfield, A. Kar, C. M. Wong and A. N. Chiaramonti, *Anal. Bioanal. Chem.*, 2013, **405**, 8207–8213.
18 J. H. Lehman, M. Terrones, V. Meunier, E. Mansfield and K. E. Hurst, *Carbon*, 2011, **49**, 2581–2602.
19 A. K. O. Åslund, E. Sulheim, E. Von Haartman, H. Baghirov, N. Starr, M. Kva, S. Lelu, D. Scurr, C. D. L. Davies, R. Schmid and Y. Mørch, *Mol. Pharmaceutics*, 2017, **14**, 2560–2569.
20 V. Atakan, C. Chen, R. Paul and R. E. Riman, *Anal. Chem.*, 2008, **80**, 6626–6632.
21 M. C. Burleigh, M. A. Markowitz, M. S. Spector and B. P. Gaber, *J. Phys. Chem. B*, 2001, **105**, 9935–9942.
22 D. Loof, M. Hiller, H. Oschkinat and K. Koschek, *Materials*, 2016, **9**, 415.
23 M. Liang, I. Lin, M. R. Whittaker, R. F. Minchin, M. J. Monteiro and I. Toth, *ACS Nano*, 2010, **4**, 403–413.
24 F. M. Wisser, M. Abele, M. Gasthauer, K. Müller, N. Moszner and G. Kickelbick, *J. Colloid Interface Sci.*, 2012, **374**, 77–82.
25 K. B. Sebby and E. Mansfield, *Anal. Bioanal. Chem.*, 2015, **407**, 2913–2922.
26 D. Das, Y. Yang, J. S. O'Brien, D. Breznan, S. Nimesh, S. Bernatchez, M. Hill, A. Sayari, R. Vincent and P. J. Kumararathasan, *Nanomaterials*, 2014, **2014**, 176015.
27 S. E. Lehman, I. A. Mudunkotuwa, V. H. Grassian and S. C. Larsen, *Langmuir*, 2016, **32**, 731–742.
28 H.-T. Lu, *Colloid J.*, 2013, **75**, 311–318.
29 C. I. C. Crucho, C. Baleizao and J. P. S. Farinha, *Anal. Chem.*, 2017, **89**, 681–687.
30 D. N. Mangos, T. Nakanishi and D. A. Lewis, *Sci. Technol. Adv. Mater.*, 2014, **15**, 015002.
31 A. M. Clemments, P. Botella and C. C. Landry, *ACS Appl. Mater. Interfaces*, 2015, **7**, 21682–21689.
32 Z. Chen, K. J. Ziegler, J. Shaver, R. H. Hauge and R. E. Smalley, *J. Phys. Chem. B*, 2006, **110**, 11624–11627.
33 D. R. Hristov, L. Rocks, P. M. Kelly, S. S. Thomas, A. S. Pitek, P. Verderio, E. Mahon and K. A. Dawson, *Sci. Rep.*, 2015, **5**, 17040.
34 S. Li, Q. Wan, Z. Qin, Y. Fu and Y. Gu, *Langmuir*, 2015, **31**, 824–832.
35 S. Li, Q. Wan, Z. Qin, Y. Fu and Y. Gu, *J. Therm. Anal. Calorim.*, 2019, **136**, 1895–1904.
36 A. Van Blaaderen, J. Van Geest and A. J. Vrij, *Colloid Interface Sci.*, 1992, **154**, 481–501.
37 J. Farrando-Perez, C. Lopez, J. Silvestre-Albero and F. Gallego-Gomez, *J. Phys. Chem. C*, 2018, **122**, 22008–22017.
38 L. T. Zhuravlev, *Langmuir*, 1987, **3**, 316–318.
39 H. G. Schild, *J. Polym. Sci., Part A: Polym. Chem.*, 1993, **31**, 1629–1632.
40 A. Brinkmann, M. Raza and J. Melanson, *Metrologia*, 2019, **56**, 024002.
41 S. Akoka, L. Barantin and M. Trierweiler, *Anal. Chem.*, 1999, **71**, 2554–2557.
42 C. Jaeger and F. Hemmann, *Solid State Nucl. Magn. Reson.*, 2014, **57–58**, 22–28.